Transfer of hydrophobic ZnO nanocrystals to water: an investigation of the transfer mechanism and luminescent properties

Javier Rubio-Garcia, Anass Dazzazi, Yannick Coppel, Patrice Mascalchi, Laurence Salomé, Ahmed Bouhaouss, Myrtil L. Kahn, Fabienne Gauffre

Transfer of Hydrophobic ZnO Nanocrystals to Water: an Investigation of the Transfer Mechanism and Luminescent Properties

Javier Rubio Garcia [a,b] , Anass Dazazzi[a,b,c] , Yannick Coppel[a], Patrice Mascalchi[d], Laurence Salomé[d], Ahmed Bouhaouss[c], Myrtil L. Kahn*[a], and Fabienne Gauffre*[e]

We investigated the "interdigitated double layer" strategy, with the objective to transfer to water hydrophobic photoluminescent ZnO nanocrystals (Ncs) stabilized by a hydrophobic ligand (octylamine). This strategy relies on the formation of a double layer around the Ncs by interdigitation of an added surfactant within the alkyl chains of the pristine ligand. Various surfactants were evaluated and surprisingly, transfer could only be achieved with a limited choice of molecular structures. Among them, the family of glycolic acid ethoxylate ethers surfactant yielded transfers up to 60%. The molecular organization of the organic coating in water was characterized using dynamic light scattering, photoluminescence and NMR (including DOSY and NOESY). Our results suggest that the success of this transfer strategy depends on a subtle interplay of interactions between the added surfactant, the ligand and the surface of the Nc. The ZnO Ncs exhibit a strong luminescence in water.

Introduction

The recent development of nanoparticles (Nps) with photoluminescent properties has opened new perspectives in the field of sensing and imaging technologies. Intense research activity is devoted to the elaboration of new luminescent semi-conducting nanocrystals (quantum dots, QD). Various physical and chemical procedures were proposed, enabling access to a large variety of materials. The chemical methods appear to be of particular interest since they offer the potential of facile scale-up and occur at lower temperatures than physical methods. Some materials may be synthesized either in water or in organic solvent but so far, better shape control and higher crystallinity are obtained in organic solvents.[1]

The most studied luminescent nanomaterials are QD such as CdSe, CdTe, InP or InAs. Indeed, they combine the advantages of high quantum yields (QY) and narrow emission band.[1,2] However, the release of severely toxic ions from these materials is a serious disadvantage for their use for *in vivo* imaging. Particularly, cadmium is one of the most toxic metals known to man with major health consequences.[3] Therefore, there is a need to develop luminescent nanocrystals (Ncs) with improved compatibility with living systems. In this context, attention is paid to ZnO semiconducting Ncs as an alternative material compatible with living organisms, even though they still offer relatively poor QY and a lack of control of their optical properties.[4-6]

We have previously evidenced the interest of organometallic complexes for the preparation of metal oxide Nps of controlled size and shape.[7-9] Particularly, luminescent ZnO Ncs were synthesized by a very simple organometallic procedure operated at room temperature.[10,11] In this procedure, the very exothermic reaction of an organometallic precursor with water produces crystalline zinc oxide. Crystal growth is controlled by ligands, typically an alkyl amine or a mixture of alkyl amine and fatty acids. This synthesis yields well-crystallized Nps whose size (typically 2-4 nm) can be varied by tuning the reaction conditions. Nanorods can also be obtained.[12] These luminescent Ncs appear to be good candidates for applications such as imaging due to their thermodynamic and air stabilities. However, the general drawback of the organometallic procedures is that they yield hydrophobic Ncs coated with a layer of alkyl ligands. Thus, a prerequisite for biomedical or other water-based applications is to modify the original hydrophobic layer for a hydrophilic one.

The most common strategy to convert hydrophobic Nps to hydrophilic ones consists in the displacement of the original ligand by hydrophilic compounds. Best results are obtained using hydrophilic ligands with multiple and strong binding, such as polyelectrolytes (or oligomers).[13-17] Encapsulation of the hydrophobic Nps within a polymer or silica shell is also an attractive method, which may provide protection against chemical degradation.[18, 19] However, these methods involve a strong alteration of the Np surface which often results in the alteration of their optical properties.[20-23] An alternative strategy was proposed, based on the encapsulation of the NPs within surfactant aggregates.[24-31] This strategy was successfully applied to QD

without changing their optical properties.[26, 27] It is generally accepted that the added surfactant interacts with the pristine ligands *via* non specific Van der Waals interactions, suggesting that this strategy could universally apply to all types of hydrophobic Nps and surfactants. For example, Yang and coworkers demonstrated that CdTe Ncs coated with the double chain DODAB (dimethyldioctadecylammonium bromide) were efficiently transferred into water, using surfactants with various lengths and head groups.[32] Some authors stated that the hydrophobic Nps are merely embedded within micelles of the added surfactant without perturbing the micellar structure,[27] while others evoked the formation of an interdigitated double layer between the alkyl chain of the surfactant and the alkyl ligands.[24, 31] However, to date, there has been no investigation of the molecular organization of the hydrophilic coating.

In an effort to produce functional Nps both water-soluble and of high quality, we have recently proposed the use of polyethylene glycol (PEG) based ligands directly in the organometallic synthesis. Indeed, PEG is soluble in all types of polar solvent, including THF, dichloromethane and water yielding multi-soluble metal and metal oxide Nps in a one step procedure.[33, 34] Here, we report an alternative strategy, based on the addition of a new surfactant to ZnO Ncs pre-formed in the presence of octylamine. Single chain surfactants with various non-ionic, anionic or cationic polar groups were evaluated, and we observed that the transfer could be obtained only with long chain alkyl ether of glycolic acid. An insight of the molecular organization of the organic coating was provided using dynamic light scattering, photoluminescence and NMR (DOSY, NOESY) measurements. The optical properties (absorbance and luminescence) of the Ncs after transfer to water were compared to the ones of the pristine ZnO Ncs in organic solvent. Importantly, the Ncs could be transferred to a buffer –an essential step to envisage any biological application– and observed using a wide field fluorescence microscope.

Results and discussion.

The hydrophobic ZnO Ncs were synthesized using octylamine (OA) as a stabilizing agent, following a well established procedure (Figure 1).[10] The synthesis is achieved at room temperature, taking advantage of the very exothermic reaction of water with the organometallic zinc precursor, bis-cyclohexyl zinc, [$Zn(Cy)_2$]. Briefly, OA was mixed with [$Zn(Cy)_2$] (OA/Zn=1), typically in THF, toluene or dichloromethane, under an inert atmosphere. Water was then introduced in the vessel, either in a controlled way or simply by opening the vessel to the air. Interestingly, cyclohexyl evaporates easily during the synthesis or on solvent removal and no other by-products are formed. Therefore, OA is the only organic moiety present in solution. Well-crystallized ZnO Nps of about 3-4 nm were obtained. Nanorods can also be obtained in pure OA. Typical TEM pictures of the isotropic Ncs and of nanorods are displayed Figure 1. Two main broad emission bands are observed in the visible range: one (blue) centered at 440 nm (~2.82 eV) for an excitation ranging from 360 to 420 nm (~3.45 to 2.95 eV) and the second one, (yellow) centered at 580 nm (~2.14 eV) for an excitation range of 280 to 360 nm (~4.43 to 3.45 eV), respectively (Figure 1). The emission properties of these nanocrystals were previously described in details by Kahn et al.[35]The yellow luminescence of ZnO Ncs is frequently reported in the literature and results from oxygen vacancies in the crystalline structure.[36] The presence of a second emission at higher energies was also observed, but at various wavelengths and its origin is still debated.[37-40] We demonstrated that the observed blue emission is due to an electronic density increase at the surface of the Ncs through the electron pair provided by the amine ligand.[41, 42] It is therefore of paramount importance to keep the amine ligands at the NP surface to maintain their attractive optical properties. Thus, the so-called "interdigitated double layer" strategy was preferred. In most reported procedures, the new surfactant is added to an organic solution of the Nps, which are further precipitated and recovered as a powder. The resulting double-layer coated Nps are hydrophilic.[26, 27, 43] However, precipitated Nps do not always readily redisperse. In order to avoid the precipitation step, we decided to transfer the Ncs *via* the emulsion formation approach.[32] Typically, a small volume (*ca.* 1/10) of a concentrated solution of the ZnO Ncs in dichloromethane was added to an aqueous solution of the surfactant. The mixture was vigorously stirred in order to form an emulsion and the flask left uncovered to allow for the evaporation of the dichloromethane. After evaporation of the organic solvent, a small amount of insoluble material adsorbed on the wall of the vials was observed. The amount of Ncs solubilized in the aqueous phase was evaluated from measurements of the absorbance (see supp Info).

Influence of the molecular structure of the surfactant on the transfer process.

Following the "interdigitated double layer" strategy, a series of anionic and cationic surfactants, all with an alkyl chain length of *ca.* 12 carbon atoms were evaluated, namely: N-dodecyl pyridinium chloride, lauric acid, lauryl sodium sulfate, polyoxyethylene lauryl ether ($C_{12}E_4$) and Lauryl-5 (Figure 2). Only Lauryl-5 led to a transparent water solution after the transfer procedure. The absorbance spectra display moreover a clear evidence of the presence of ZnO Ncs in the water solution. However, the other surfactants yielded more or less turbid aqueous phases with no significant absorbance related to ZnO Ncs. These results clearly demonstrate that not any surfactant could efficiently transfer the ZnO/OA Ncs in water, contrasting with the proposed mechanism of the "interdigitated double layer" method hypothesizing the formation of an interdigitated double layer *via* non specific Van der Waals interactions. In addition, the presence of micelles in the aqueous solution does not necessarily enable the transfer, since the Ncs were not transferred into a $C_{12}E_4$ solution at a concentration (3 mmoles.L^{-1}) largely exceeding the CMC (~ 0.1 mmoles.L^{-1}).

The molecular structure of the polar part of the surfactant obviously played a predominant role, suggesting a specific interaction of the surfactant either with OA or with the ZnO Nc surface. Importantly, we have previously demonstrated by NMR spectroscopy that a large fraction of the capping OA is in fast exchange between the liquid phase and the Ncs surface while another is strongly bonded (at the NMR time scale).[44] Similar observations were reported by different groups for CdSe QD synthesized in the presence of TOP or TOPO ligands.[45, 46] Surfactant adsorption can involve various mechanisms such as

covalent, electrostatic, hydrogen bonding with the surface groups or Van der Waals interactions between hydrophobic chains.[27, 47] Entropic effects arising from the desolvation of the surface or of the polar group of the surfactant also have to be considered.[48] On large surfaces (*e.g.* porous silica) several regime of adsorption including individual molecules, patches of laterally interacting molecules and hemi-micelles and bicontinuous double layer are observed, depending on the surfactant and on its concentration.[49, 50] However little is known in the case of adsorption on nanoparticles. Metal oxide surfaces are generally charged in water, the sign and extent of charging being controlled mainly by the adsorption of H^+ or OH^- ions on amphoteric sites. The isoelectric point of ZnO in water is reached at *ca.* pH=9.[51] In the present case, we observed that neither the anionic (SDS) nor the cationic (C_{12}PyCl) surfactants enabled an efficient transfer, indicating that pure electrostatic interaction is not the main driving force. Poly(oxyethylene) groups were reported to link the surface of metal oxide *via* hydrogen bonds.[52] However transfer with $C_{12}E_4$ was not successful in our case. Interestingly, a carboxyl function or oxyethylene groups alone (respectively in lauric acid and $C_{12}E_4$) did not enable the transfer whereas the combination of both did (Lauryl-5). This suggests that the acid function lowers the pH value at the Nc surface, displacing the Zn-OH/Zn-O^- surface equilibrium toward the -OH form, thus favoring hydrogen bonding with the oxyethylene groups of the surfactant. The formation of an ion pair between octylamine and acidic surfactants has also to be considered, however this should lead to a stabilizing effect both for Lauric acid and Lauryl-5.

These results led us to examine more surfactants with ethoxylated glycolic acid head groups (see Figure 3b for the molecular structures). After the transfer procedures using 3 mM solutions of Lauryl-2, Lauryl-5 and Lauryl-10, all the aqueous phases were somewhat turbid and were filtrated. Measurement of the absorbance showed that the ZnO Ncs were successfully transferred to water (~30%) when Lauryl-2 and Lauryl-5 were used (Figure 3a). In contrast, almost no transfer occurred when using Lauryl-10. This can be attributed to the higher solubility of Lauryl-10 in water compared to the ones of Lauryl-2 and Lauryl-5. This higher solubility necessarily decreases the tendency of Lauryl-10 to adsorb at the solid/liquid interface. In addition, ethoxylated surfactants have the tendency to adsorb with the ethoxy groups parallel to the surface, so that the maximum concentration adsorption decreases linearly with the number of ethoxy groups.[50] The influence of the solubility of the surfactant can also be investigated by comparing surfactants with a similar polar group but different alkyl chains. In this context, we selected an oleyl based surfactant (*i.e.* Oleyl-10) for comparison with Lauryl-10. The oleyl chain was chosen to avoid the low melting point temperature of longer chain surfactants (Figure 3). Interestingly, the aqueous ZnO solutions obtained using Oleyl-10 were transparent and did not require to be filtrated. In addition, more than 60% of the Nps were transferred to water, which compares with the best results reported so far.[53] Importantly, ZnO/OA nanorods synthesized using a slightly modified procedure (see experimental section) were also successfully transfered (supporting info, Figure S2), indicating no significant influence of the shape.

To summarize, the choice of the surfactant structure and particularly of its polar part appears of crucial importance. Particularly, the combination of both a carboxyl and ethoxyl groups in the surfactant structure enables an efficient transfer. These results suggest that a specific interaction between the surfactant head group and the ZnO Ncs surface is involved in the building up of the organic corona surrounding the Ncs.

Characterization of the organic coating by DLS, zeta potential measurements, and NMR spectroscopy.

In the following, all transfer experiments were achieved using Oleyl-10, which gave the best results in terms of transfer efficiency. After transfer, the pH value is typically in the range 6.5-7. No significant change in their absorbance could be observed during the first three weeks when the solutions were stored at 10 °C in the dark. After this period, the Nps started dissolving (ESI, Figure S3). Interestingly, no troubling or precipitation was observed when NaCl was added up to 0.2 moles.L^{-1} which compares to physiological conditions. This observation clearly indicated that the Nps were colloidally stable in conditions where electrostatic stabilization is shielded (ESI, Figure S4).[28] This certainly results from the steric stabilization provided by the ethylene oxide groups in the polar head of Oleyl-10. TEM observations of the ZnO Ncs before and after transfer were conducted (Figure 4). In water, the presence of patches of organic material reduced the contrast, but the morphology of the ZnO Ncs (diameter 4.5 ±1.5 nm) is not significantly modified.

Dynamic light scattering (DLS), zeta potential measurements, and NMR spectroscopy were used to probe the organic coating of the Ncs.[54] The values of the hydrodynamic diameters and zeta potentials were respectively D_h = 10.7 nm and ζ = 12.3 mV for ZnO/OA in dichloromethane and D_h = 14.1 nm and ζ = -40.3 mV for ZnO/OA/Oleyl-10 in water. These results are consistent with the building up of a double layer with a strong negative net charge.

A first set of NMR experiments was performed either on the ligand alone (*i.e.* OA or Oleyl-10 in water) or on mixtures of the ligands (*i.e.* both OA and Oleyl-10 in water) in the absence of ZnO Ncs. Figure **5** shows the relevant ^{1}H NMR resonances of a) a 8 mM OA water solution, b) a 2 mM Oleyl-10 water solution and c) a mixture of OA (8 mM) and of Oleyl-10 (2 mM). The full spectra are reported in ESI, Figure S6. The signal corresponding to the protons in the alpha (α-CH_2) and beta (β-CH_2) positions of the amine group were significantly affected by the presence of Oleyl-10, shifting from 2.61 ppm to 2.86 ppm and from 1.41 to 1.57 ppm, respectively. In contrast, no clear change was observed for the Oleyl-10 resonances (modification of the resonance values lower than 5 Hz). The observed shifts in OA resonances may have two origins: (i) the formation of an ammonium carboxylate, and/or (ii) the insertion of OA molecules within Oleyl-10 aggregates. Since OA is in excess compared to Oleyl-10 (4 eq.), the presence of a single set of resonance signals most probably correspond to a fast equilibrium (at the NMR time scale) between free OA and OA in interaction with Oleyl-10.

The diffusion coefficients of OA and Oleyl-10 were measured by DOSY (diffusion ordered spectroscopy). When one moiety exists under states with different dynamics (e.g. monomeric,

adsorbed onto particle surface and within micelles) and if the equilibrium between some of these states is fast compared to the NMR time scale, then the observed diffusion coefficient is an averaged value, weighted by the molar fractions of the different states.[55] For instance, in the case of a micellar solution with a "rapid" monomer–micelle equilibrium the observed diffusion coefficient (D) is equal to $D = x_{mon} D_{mon} + x_{mic} D_{mic}$, where x and D correspond to the molecular fractions and the diffusion coefficients, and the indices "mon" and "mic" refer to the monomeric surfactant and the surfactant within micelles, respectively. If the equilibrium is "slow", then two different diffusion coefficients corresponding to the monomer and micelle states are observed. DOSY measurements of aqueous solutions of OA (8 mM) or Oleyl-10 (2 mM) yielded only one diffusion coefficient for each species, respectively $4.9 \pm 0.2 \times 10^{-10}$ m^2/s and $0.37 \pm 0.03 \times 10^{-10}$ m^2/s. The value obtained for Oleyl-10 clearly indicates that, at this concentration, the solution is mainly composed of micelles. The value obtained for OA, is one order of magnitude larger, and compares to monomeric species. For comparison, the self-diffusion coefficient of monomeric OA is expected to be *ca*. 8.9×10^{-10} m^2/s in water taking into account the self-diffusion coefficient of monomeric OA in toluene ($16.6 \pm 0.2 \times 10^{-10}$ m^2/s) and the difference of viscosities between toluene and water (0.57 mPa.s and 1 mPa.s, respectively at 22°C). This suggests that the majority of OA is under monomeric form, in fast equilibrium with a limited amount of micelles. For the OA/Oleyl-10 mixture, the diffusion coefficients of OA and Oleyl-10 are $3.7 \pm 0.3 \times 10^{-10}$ m^2/s and $0.39 \pm 0.04 \times 10^{-10}$ m^2/s, respectively. The diffusion coefficient of Oleyl-10 was almost unmodified whereas the diffusion coefficient of OA slightly decreased. This observation suggested an interaction between OA and the Oleyl-10 micelles, but could also result from the formation of ammonium carboxylate ion pairs in solution between OA and Oleyl-10. DOSY experiments were also achieved at pH 12 (forbidding the formation of an ammonium carboxylate) and yielded similar diffusion coefficient values (*i.e.* $3.8 \pm 0.3 \times 10^{-10}$ m^2/s and $0.38 \pm 0.04 \times 10^{-10}$ m^2/s for OA and Oleyl-10, respectively) confirming that the slowing down of OA diffusion, was not related to the formation of an ion pair. When ZnO Ncs synthesized in the presence of 8 mM of OA were transferred to D_2O using 2 mM of Oleyl-10, the ^1H NMR spectra of this solution (Figure **5**d) evidenced resonance shifts and broadening of the α-CH_2 and β-CH_2 OA signals (26 Hz and 11 Hz, respectively) compared to the ones obtained for the same ligand mixture but in the absence of ZnO Ncs (vide intra). On the other hand, no significant modification of the Oleyl-10 resonances was detected in the presence of the ZnO/OA Ncs. When the concentration of Oleyl-10 decreased from 2 to 0.5 mM, sharpening of the α-CH_2 and β-CH_2 OA signals were observed but no significant chemical shift were detected (ESI, Figure S7). Regardless of the sample, the diffusion coefficient of Oleyl-10 remained constant and equal to the one measured in solutions of Oleyl-10 alone ($D_{Oleyl\text{-}10} = 0.39 \pm 0.04 \times 10^{-10}$ m^2/s).[56] The diffusion coefficient of OA, slightly increased when the concentrations of Oleyl-10 decreases ($D_{OA} = 4.4 \pm 0.3 \times 10^{-10}$, $4.8 \pm 0.3 \times 10^{-10}$ and $5.0 \pm 0.3 \times 10^{-10}$ m^2/s for 2, 1 and 0.5 mM Oleyl-10, respectively). These values were slightly higher than the one measured for the same mixture but in the absence of ZnO Ncs ($D_{OA} = 3.8 \pm 0.3 \times 10^{-10}$ m^2/s) but remained smaller than the one of the OA micellar solution ($D_{OA} = 4.9 \pm 0.2 \times 10^{-10}$ m^2/s). Altogether, these DOSY experiments indicate that OA is highly dynamic and is in fast exchange between a slow motion state (*i.e.* micelles and/or OA on the Np surface) and a monomer state. The fraction of OA in the slow state increased with the concentration of Oleyl-10, suggesting the formation of mixed aggregates of OA and Oleyl-10. Conversely, the low diffusion coefficients measured for Oleyl-10 show that in all samples only a negligible fraction of Oleyl-10 molecules were in the monomeric state.

NOESY experiments showed negative NOE for OA and Oleyl-10 regardless of the sample containing ZnO (Figure **6**). In the case of Oleyl-10, this is not surprising as the diffusion coefficient indicated that Oleyl-10 acted as a large molecule. On the other hand, OA showed also negative NOEs even though its diffusion coefficient was ten times faster than the one of Oleyl-10. Such large negative NOEs were measured recently for the pristine ZnO Ncs in the presence of OA in toluene.[44] They were attributed to transferred NOEs in conditions of fast exchange between OA with slow motion at the surface of the ZnO Ncs and OA monomer with fast motions.[54] Furthermore, the NOE cross peaks of OA have stronger amplitudes than the ones of Oleyl-10 (about 5 times for 2mM Oleyl-10). This observation indicates a preferential interaction of OA for the ZnO Nps. Indeed, if OA were preferentially interacting with Oleyl-10 aggregates, OA should have NOEs with amplitude equal or even weaker than the Oleyl-10 ones. This result is confirmed by the absence of negative NOE for mixtures of OA and Oleyl-10 in D_2O (observation of zero quantum artifact[54]) in the absence of ZnO Ncs (Figure **6**). The NOE cross peak between protons in alpha and beta positions of the amine group integrated for 0.04, 0.06 and 0.36 compare to the diagonal peak of alpha protons set to 1, with 0.5, 1 and 2 mM Oleyl-10, respectively. The increase of negative NOE amplitude with the concentration of Oleyl-10 shows a stronger interaction of OA with the ZnO Ncs as the concentration of Oleyl-10 increases. No clear signature of intermolecular NOE between OA and Oleyl-10 could be observed. However, the strong superposition of the proton signals of methylene and methyl from the alkyl chains of OA and of Oleyl-10 could make them difficult to observe.

DOSY and NOESY experiments performed for the same ZnO/OA/Oleyl-10 system at pH 12 exhibited very similar results, namely : i) a slow diffusion coefficient value for Oleyl-10 ($0.37 \pm 0.04 \times 10^{-10}$ m^2/s), ii) a relatively fast diffusion coefficient for OA, slightly increasing with decreasing the concentration of Oleyl-10 ($D_{OA} = 3.3 \pm 0.3 \times 10^{-10}$, $3.5 \pm 0.3 \times 10^{-10}$ and $4.2 \pm 0.3 \times 10^{-10}$ m^2/s for 2, 1 and 0.5 mM of Oleyl-10, respectively), iii) negative NOEs are observed for both OA and Oleyl-10 with a stronger amplitude for OA (Transferred NOEs ; ESI, Figure S8).

Both the decrease in the diffusion coefficient of OA and the increase of negative NOE amplitude with increasing the concentration of Oleyl-10 suggest a synergistic effect of OA and Oleyl-10 promoting the adsorption of OA (and possibly of Oleyl-10) at the ZnO Ncs surface. It has been reported that surfactant adsorption can be either enhanced or decreased using mixtures of oppositely charged surfactants, depending on the surface charge and on the surfactants propensity to form mixed micelles.[57] Since ZnO Ncs and OA are positively charged, and Oleyl-10 negatively

charged, co-adsorption of Oleyl-10 with OA on the nanocrystal surfaces reduces the overall surface charge, thus allowing more OA to adsorb.

Altogether, DLS, zeta potential and NMR measurements strongly suggest that the transfer of the ZnO Ncs occurs *via* the formation of an interdigitated double layer. The localization of OA and Oleyl-10 within the double layer remains difficult to determine. ATR and FT-IR spectra were also recorded but were not informative since no significant difference was observed between mixtures of OA and Oleyl-10 and the ZnO/OA/Oleyl-10 solution after transfer. However, the negative overall surface charge suggests that the outer layer contains predominantly Oleyl-10. The presence of transferred NOE for OA demonstrates that a fraction of the OA is less mobile than Oleyl-10, which is attributed to OA molecules in strong interaction with the Np surface. Such results are in agreement with the optical properties recorded in water (vide intra). Previous study on ZnO NPs stabilized only by the amine ligands has shown that the transferred NOEs are not due to an exchange involving the ligands directly coordinated at the NP surface (first shell) but to an exchange between a second ligand shell surrounding the NPs and the mobile ligands in solution.[54] The first ligand shell (*i.e.* the one corresponding to the ligands directly adsorbed on the NPs) is not well characterized at this stage. This first shell involved only a small amount of molecules (only few percent[58]) that probably encounter broadening effects making them difficult to observe or to differentiate from the slowly mobile Oleyl-10 molecules (signal superposition). The first shell can be composed of strongly bonded OA[54] but coordination of carboxylate at the ZnO Ncs surface was also evidenced previously. [59] Consequently, the first ligand shell of the ZnO/OA/Oleyl-10 system in water can also potentially contain Oleyl-10 molecules grafted on its surface.

Optical properties of the ZnO Ncs after their transfer to water. Figure 7a displays a comparison of the optical properties (absorbance and emission) before and after transfer. The absorbance spectra of the aqueous solution were normalized to take into account the loss of Ncs during transfer. The normalization factor (x 2.1) was chosen so that the steep increase in absorbance between 3.28 eV (378 nm) and 3.54 eV (350 nm) was the same for the aqueous and the dichloromethane solutions. Even though the aqueous samples looked transparent by naked eyes (Figure 7b), some scattering was observed in the UV range of the spectra. The normalization factor is however little influenced by light scattering. Importantly, the overall profiles and particularly the onset of absorbance of ZnO Ncs (376 nm, 3.30eV) were not modified by the transfer procedure. At high energies however, the discrepancy between both spectra is more pronounced, due to an increase of light scattering in the UV domain.

The nanocrystals were strongly luminescent in water (Figure 7c-d). Compared to the pristine Ncs, both the QY and the relative intensity of the blue and yellow emissions were modified. The spectra recorded for λ_{exc} = 360 nm (3.44 eV) are displayed Figure 7b (for other excitation wavelengths, see ESI Figure S5). In order to compare the organic and aqueous solution emissions, the spectra of the aqueous solutions were multiplied by the same factor as for the absorption spectra. The QY of the pristine ZnO nanocrystals in dichloromethane was *ca*. 15% for excitations within the range 320-360 nm (3.44-3.87 eV), where only yellow light is emitted. It appeared that the QY associated to the yellow band was enhanced (by a factor up to 1.6) in water regardless the excitation wavelength. The behaviour of the blue emission was more complex. In the low energy excitation range (420-365 nm, 2.95-3.4-eV), the QY associated with the blue emission was slightly inhibited in water. However, whereas the blue emission promptly disappeared for excitation energies higher than 3.4 eV (365 nm) for the pristine ZnO Ncs in dichloromethane, it was present in water up to 3.87 eV (λ_{exc} = 320 nm). Based on previous experiments showing the role of amine ligands on the blue emission,[60] we propose that this behaviour is related to differences in the coordination strength and/or amount of the amine bound to the ZnO surface in water and in dicholoromethane. The luminescence properties remained stable under UV irradiation for several hours. Importantly, the Ncs could be transferred to a buffer –an essential step to envisage any biological application– and observed using a wide field fluorescence microscope (Figure 7d).

Conclusion.

Hydrophobic ZnO Ncs were efficiently transferred to water using the "interdigitated double layer" strategy. We demonstrated that the practical implementation of this strategy is not as straightforward as it is usually pictured and that only a few surfactants selected from the family of glycolic acid ether ethoxylates were indeed efficient. Using a complementary set of techniques including DLS and NMR spectroscopy, we demonstrated that the stabilization of the ZnO Ncs involves the formation of an organic layer comprising the pristine ligand (octylamine) and the glycolic acid based surfactants. In addition, a specific interaction between the surfactant and the nanoparticle surface is most likely involved. The water soluble Ncs exhibited good colloidal stability and strong photoluminescence, enabling prospects for use as cheap and safe photoluminescent labels. Further work is underway to extend this strategy to other oxides stabilized with alkylamine ligands such as magnetic iron oxide nanoparticles.

Experimental section.

Material. THF was purchased from Aldrich and purified by distillation before use as solvent for the synthesis of the ZnO Ncs. The THF used to solubilise the Ncs after the synthesis was not distillated. All surfactants used were purchased from Sigma or Aldrich and used without further purification. Commercial names of the ethoxylated surfactants are: Brij 30 (Sigma; $C_{12}E_4$), glycolic acid lauryl ether (Aldrich; M_n=360; 460 and 690); glycolic acid ethoxylate oleyl ether (Aldrich; M_n=700).

Synthetic Procedures. Synthesis of the Zn precursor and of the ZnO nanocrystals were performed as described in ref [61]. A THF solution containing (57.9 mg, 0.25 mmoles) of biscyclohexyl zinc and 1eq. of octylamine was first prepared from freshly distilled THF in a glove box under argon. After extraction from the glove box, the solution was exposed to ambient moisture by opening the Schlenk tube. A powder is obtained after solvent evaporation, which readily dispersed into organic solvents such as dichloromethane.

Transfer toward water. To the powder sample resulting from the synthesis, 10 mL of dicholoromethane was added and the sample was stirred to yield a transparent solution. Then, 250µL of this solution was added to 2mL of water, forming an emulsion that was vigorously stirred. The vial was then open to air under gentle stir until evaporation of the dichloromethane was completed. The aqueous solutions were not filtrated prior to optical measurements, unless otherwise stated. It was verified using NMR that after evaporation the organic solvent was only present as traces (C< 0.2 mM). For determination of the yield of transfer see ESI.

TEM and optical characterization. TEM experiments were prepared by slow evaporation of droplets of colloidal solution of the different samples deposited on carbon supported copper grids. The experiments were performed on a JEOL 1011 operating at 100 kV. All optical measurements were achieved using quartz cells of optical pathway 1 cm. Emission spectra were recorded using a Jobin–Yvon spectrofluorometer. Normalized absorbance spectra (fig 5) were obtained by introducing a multiplication factor (x2.3 to the data in water) to adjust the absorbance values at 360 nm. Ncs diluted in Tris buffer were observed through a Zeiss Plan Apochromat 63x/1.40 Oil objective on an Zeiss Axioplan 2 microscope, using an X CITE 120 light source containing a mercury vapor short arc lamp (excitation filter 365/10, emission filter HQ595lp). Images were collected by a Cascade II 512 EM-CCD camera (Roper Scientific).

NMR. For NMR samples the transfer procedure was achieved using D_2O solutions of surfactants. The pH was not controlled or was adjusted to pH~12 by addition of small volumes of a solution of NaOH in D_2O. 1D and 2D ^1H NMR experiments were recorded on a Bruker Avance 500 spectrometer equipped with a 5 mm triple resonance inverse Z-gradient probe. All chemical shifts are relative to TMS. All diffusion measurements were made using the stimulated echo pulse sequence with bipolar gradient pulses. The 2D NOESY measurements were done with a mixing time of 100 ms.

Notes and references

The authors acknowledge the financial support of the EU through the Nanotool project (EST n°MEST-CT-2005-020195) and of the LIA and the CNRS-CNRST.

[a] *CNRS, LCC (Laboratoire de Chimie de Coordination), 205 route de Narbonne, F-31077 Toulouse, France. Fax: +33 5 6155 3003;Tel: +33 5 6133 3130 E-mail: myrtil.kahn@lcc-toulouse.fr*

[b] *Laboratoire des IMRCP, CNRS/Universite´ de Toulouse, 31062 Toulouse Cedex 09, France. E-mail: dazzazi@chimie.ups-tlse.fr*

[c] *Laboratoire de Chimie Physique Générale des Matériaux, Nanomatériaux et Environnement, Faculté des sciences, université Mohammed V Agdal, Rabat, Maroc.*

[d] *IPBS (Institut de Pharmacologie et de Biologie Structurale), CNRS/Université de Toulouse; 205 route de Narbonne, F-31077 Toulouse, France*

[e] *Institut des Sciences Chimiques de Rennes, UMR 6226 (CNRS/UR1), Campus Beaulieu , CS 74205, 35042 Rennes Cedex, France. Tel: 33 +2 2323 6398; E-mail: fabienne.gauffre@univ-rennes1.fr*

† Electronic Supplementary Information (ESI) available: [details of any supplementary information available should be included here]. See DOI: 10.1039/b000000x/

‡ Footnotes should appear here. These might include comments relevant to but not central to the matter under discussion, limited experimental and spectral data, and crystallographic data.

1. P. Zrazhevskiy, M. Sena and X. Gao, *Chemical Society Reviews*, 2010, **39**.
2. T. L. Doane and C. Burda, *Chemical Society Reviews*, 2012.
3. C.-H. Lin, L. W. Chang, H. Chang, M.-H. Yang, C.-S. Yang, W.-H. Lai, W.-H. Chang and P. Lin, *Nanotechnology*, 2009, **20**, 215101.
4. X. Tang, E. S. G. Choo, L. Li, J. Ding and J. Xue, *Chemistry of Materials*, 2010, **22**, 3383-3388.
5. H.-M. Xiong, Y. Xu, Q.-G. Ren and Y.-Y. Xia, *Journal of the American Chemical Society*, 2008, **130**, 7522-7523.
6. X. Tang, E. S. G. Choo, L. Li, J. Ding and J. Xue, *Langmuir*, 2009, **25**, 5271-5275.
7. M. L. Kahn, A. Glaria, C. Pages, M. Monge, L. Saint Macary, A. Maisonnat and B. Chaudret, *Journal of Materials Chemistry*, 2009, **19**, 4044-4060.
8. A. Glaria, M. L. Kahn, A. Falqui, P. Lecante, V. Colliere, M. Respaud and B. Chaudret, *Chemphyschem*, 2008, **9**, 2035-2041.
9. A. Glaria, M. L. Kahn, P. Lecante, B. Barbara and B. Chaudret, *Chemphyschem*, 2008, **9**, 776-780.
10. M. Monge, M. L. Kahn, A. Maisonnat and B. Chaudret, *Angewandte Chemie International Edition*, 2003, **42**, 5321-5324.
11. M. L. Kahn, M. Monge, E. Snoeck, A. Maisonnat and B. Chaudret, *Small*, 2005, **1**, 221-224.
12. M. L. Kahn, M. Monge, V. Colliere, F. Senocq, A. Maisonnat and B. Chaudret, *Advanced Functional Materials*, 2005, **15**, 458-468.
13. Y. L. Xu, Y. Qin, S. Palchoudhury and Y. P. Bao, *Langmuir*, **27**, 8990-8997.
14. T. Zhang, J. Ge, Y. Hu and Y. Yin, *Nano Letters*, 2007, **7**, 3203-3207.
15. A. Dong, X. Ye, J. Chen, Y. Kang, T. Gordon, J. M. Kikkawa and C. B. Murray, *Journal of the American Chemical Society*, **133**, 998-1006.
16. N. R. Jana, N. Erathodiyil, J. Jiang and J. Y. Ying, *Langmuir*, 2010, **26**, 6503-6507.
17. H. Duan and S. Nie, *Journal of the American Chemical Society*, 2007, **129**, 3333-3338.
18. S. T. Selvan, T. T. Y. Tan, D. K. Yi and N. R. Jana, *Langmuir*, 2010, **26**, 11631-11641.
19. P. Yang, M. Ando and N. Murase, *Langmuir*, 2011, **27**, 9535-9540.
20. J. Aldana, Y. A. Wang and X. Peng, *Journal of the American Chemical Society*, 2001, **123**, 8844-8850.
21. P. Yang, M. Ando and N. Murase, *Langmuir*, 2011, **27**, 9535-9540.
22. D. R. Baker and P. V. Kamat, *Langmuir*, 2010, **26**, 11272-11276.
23. G. Kalyuzhny and R. W. Murray, *Journal of Physical Chemistry B*, 2005, **109**, 7012-7021.
24. S. Khalafalla and G. Reimers, *Magnetics, IEEE Transactions on*, 1980, **16**, 178-183.
25. X. Wu, H. Liu, J. Liu, K. N. Haley, J. A. Treadway, J. P. Larson, N. Ge, F. Peale and M. P. Bruchez, *Nat Biotech*, 2003, **21**, 41-46.
26. T. Pellegrino, L. Manna, S. Kudera, T. Liedl, D. Koktysh, A. L. Rogach, S. Keller, J. Radler, G. Natile and W. J. Parak, *Nano Letters*, 2004, **4**, 703.
27. B. Dubertret, P. Skourides, D. J. Norris, V. Noireaux, A. H. Brivanlou and A. Libchaber, *Science*, 2002, **298**, 1759-1762.
28. A. Prakash, H. Zhu, C. J. Jones, D. N. Benoit, A. Z. Ellsworth, E. L. Bryant and V. L. Colvin, *Acs Nano*, 2009, **3**, 2139-2146.

29. X. H. Gao, Y. Y. Cui, R. M. Levenson, L. W. K. Chung and S. M. Nie, *Nature Biotechnology*, 2004, **22**, 969-976.
30. N. Travert-Branger, F. Dubois, J.-P. Renault, S. Pin, B. Mahler, E. Gravel, B. Dubertret and E. Doris, *Langmuir*, **27**, 4358-4361.
31. L. Shen, P. E. Laibinis and T. A. Hatton, *Langmuir*, 1998, **15**, 447-453.
32. H. Zhang, Y. Liu, J. Zhang, H. Sun, H. Wu and B. Yang, *Langmuir*, 2008, **24**, 12730-12733.
33. J. Rubio-Garcia, Y. Coppel, P. Lecante, C. Mingotaud, B. Chaudret, F. Gauffre and M. L. Kahn, *Chemical Communications*, **47**, 988-990.
34. S. Saliba, C. V. Serrano, J. Keilitz, M. L. Kahn, C. Mingotaud, R. Haag and J. D. Marty, *Chemistry of Materials*, 2010, **22**, 6301-6309.
35. M. L. Kahn, T. Cardinal, B. Bousquet, M. Monge, V. Jubera and B. Chaudret, *ChemPhysChem*, 2006, **7**, 2392-2397.
36. A. van Dijken, E. A. Meulenkamp, D. Vanmaekelbergh and A. Meijerink, *Journal of Physical Chemistry B*, 2000, **104**, 4355-4360.
37. A. Somwangthanaroj, A. Matsumura and S. Ando, in *Zinc Oxide Materials and Devices*, eds. F. H. Teherani and C. W. Litton, 2006.
38. A. B. Djurisic and Y. H. Leung, *Small*, 2006, **2**, 944-961.
39. D. Li, Y. H. Leung, A. B. Djurisic, Z. T. Liu, M. H. Xie, S. L. Shi, S. J. Xu and W. K. Chan, *Applied Physics Letters*, 2004, **85**, 1601-1603.
40. J. Yang, X. Liu, L. Yang, Y. Wang, Y. Zhang, J. Lang, M. Gao and M. Wei, *Journal of Alloys and Compounds*, 2009, **485**, 743-746.
41. P. M. Chassaing, F. Demangeot, V. Paillard, A. Zwick, N. Combe, C. Pages, M. L. Kahn, A. Maisonnat and B. Chaudret, *Applied Physics Letters*, 2007, **91**.
42. P. M. Chassaing, F. Demangeot, V. Paillard, A. Zwick, N. Combe, C. Pages, M. L. Kahn, A. Maisonnat and B. Chaudret, *Physical Review B*, 2008, **77**.
43. S. Sun, H. Zeng, D. B. Robinson, S. Raoux, P. M. Rice, S. X. Wang and G. Li, *JACS*, 2003, **126**, 273-279.
44. Y. Coppel, G. Spataro, C. Pagès, B. Chaudret, A. Maisonnat and M. L. Kahn, *Chemistry – A European Journal*, 2012, n/a-n/a.
45. G. Kalyuzhny and R. W. Murray, *The Journal of Physical Chemistry B*, 2005, **109**, 7012-7021.
46. A. J. Morris-Cohen, M. D. Donakowski, K. E. Knowles and E. A. Weiss, *The Journal of Physical Chemistry C*, 2009, **114**, 897-906.
47. S. Sistach, K. Rahme, N. Perignon, J. D. Marty, N. L. D. Viguerie, F. Gauffre and C. Mingotaud, *Chemistry of Materials*, 2008, **20**, 1221-1223.
48. P. Somasundaran, S. Shrotri and L. Huang, *Pure and Applied Chemistry*, 1998, **70**, 621-626.
49. R. Zhang and P. Somasundaran, *Advances in Colloid and Interface Science*, 2006, **123-126**, 213-229.
50. P. L. Desbene, F. Portet and C. Treiner, *Journal of Colloid and Interface Science*, 1997, **190**, 350-356.
51. A. Degen and M. Kosec, *Journal of the European Ceramic Society*, 2000, **20**, 667-673.
52. X. Liu, J. Yang, L. Wang, X. Yang, L. Lu and X. Wang, *Materials Science and Engineering: A*, 2000, **289**, 241-245.
53. W. W. Yu, E. Chang, J. C. Falkner, J. Zhang, A. M. Al-Somali, C. M. Sayes, J. Johns, R. Drezek and V. L. Colvin, *J. Am. Chem. Soc.*, 2007, **129**, 2871-2879.
54. B. Fritzinger, I. Moreels, P. Lommens, R. Koole, Z. Hens and J. C. Martins, *Journal of the American Chemical Society*, 2009, **131**, 3024-3032.
55. E. J. Cabrita and S. Berger, *Magnetic Resonance in Chemistry*, 2002, **40**, S122-S127.
56. M. Verbrugghe, E. Cocquyt, P. Saveyn, P. Sabatino, D. Sinnaeve, J. C. Martins and P. Van der Meeren, *Journal of Pharmaceutical and Biomedical Analysis* 2010, **51**, 583-589.
57. A. Upadhyaya, E. Acosta, J. Scamehorn and D. Sabatini, *Journal of Surfactants and Detergents*, 2007, **10**, 269-277.
58. Y. Coppel, G. Spataro, V. Collière, B. Chaudret, C. Mingotaud, A. Maisonnat and M. L. Kahn, *Eur. J. Inorg. Chem.*, 2012, **in press**.
59. C. Pages, Y. Coppel, M. L. Kahn, A. Maisonnat and B. Chaudret, *Chem Phys Chem*, 2009, **10**, 2324-2344.
60. M. L. Kahn, T. Cardinal, B. Bousquet, M. Monge, V. Jubera and B. Chaudret, *Chemphyschem*, 2006, **7**, 2392-2397.
61. M. Monge, M. L. Kahn, A. Maisonnat and B. Chaudret, *Angewandte Chemie-International Edition*, 2003, **42**, 5321-5324.
62. P. Mukerjee and K. Mysels, *Critical Micelle Concentration of Aqueous Surfactant Systems*, Washington, D.C. : U.S. Dept. of Commerce, National Bureau of Standards, Washington, 1971.
63. H. Nakamura, A. Sano and K. Matsuura, *Analytical Sciences*, 1998, **14**, 379-382.
64. G. Gutierrez, J. M. Benito, J. Coca and C. Pazos, *Chemical Engineering Journal*, **162**, 201-207.

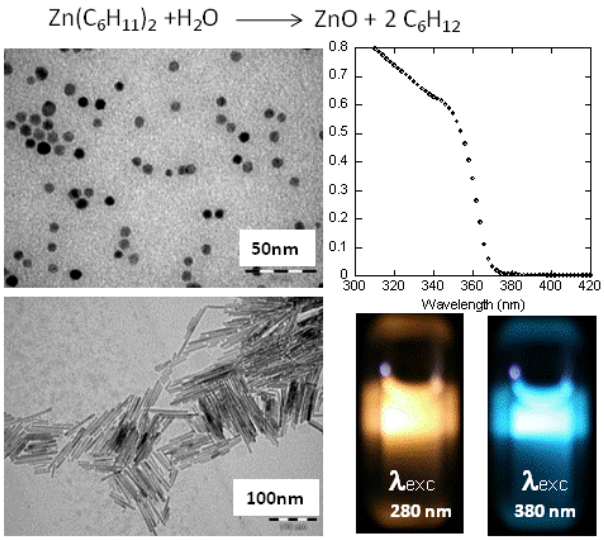

Figure 1: Summary of the main features of the hydrophobic ZnO/OA Ncs used in this study. Top: Reaction scheme of the decomposition of the organometallic precursor. Left: TEM pictures of the nanocrystals (isotropic Ncs and nanorods). Right: Absorbance spectra of isotropic Ncs in dichloromethane and pictures of same solutions under UV irradiation at 280 and 380 nm.

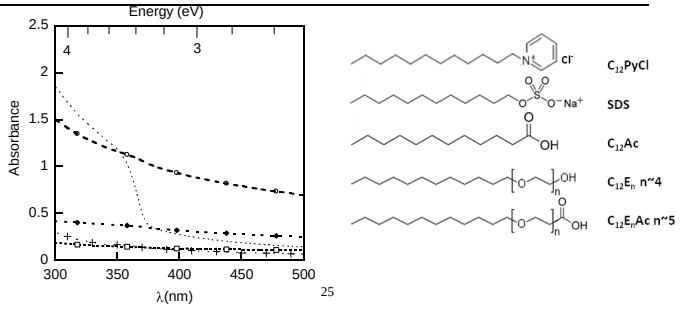

Figure 2 : Absorbance measurements of the aqueous phases after the transfer procedure using C_{12} surfactants. (o) C_{12}PyCl; (□) lauric acid; (+) $C_{12}E_4$; (♦) SDS; (…)Lauryl-5. Surfactant concentration: 3mM.

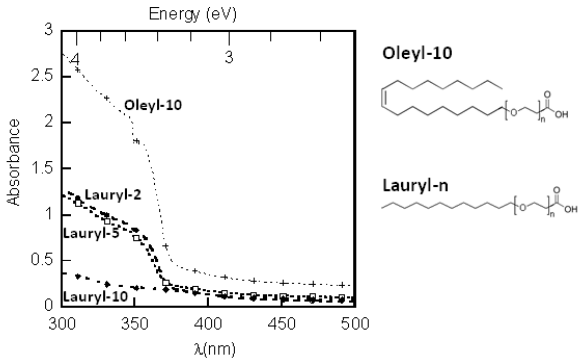

Figure 3 : Absorbance of the aqueous phase after transfer using Lauryl alkyl ethoxylate surfactants with 2, 5 and 10 oxyethylene groups and Oleyl-10. Surfactant concentration: 3mM.

Name	Abbrev.	M_n (g.mole^{-1})	CMC[a] (mmoles.L^{-1})	n
N-dodecylpyridinium chloride $CH_3(CH_2)_{11}NC_5H_5^+, Cl^-$	C_{12}PyCl	284	8-10	0
Sodium Lauryl Sulfate $CH_3(CH_2)_{11}OSO_3^-, Na^+$	SDS	288	8.3	0
Lauric acic $CH_3(CH_2)_{10}COOH$	C_{12}Ac	200	7.1[b]	0
Polyoxyethylene lauryl ether $C_{12}H_{25}(OCH_2CH_2)_4OH$	$C_{12}E_4$	362	0.09-0.1	4
Glycolic acid ethoxylate oleyl ether $CH_3(CH_2)_{5\text{-}7}C=C(CH_2)_8O(CH_2CH_2O)_nCH_2COOH$	Oleyl-10	700	0.028[c]	9.3
Glycolic acid ethoxylate lauryl ether $CH_3(CH_2)_{11\text{-}13}O(CH_2CH_2O)_nCH_2COOH$	Lauryl-2	360	>0.1[d]	2.3
	Lauryl-5	460	>0.1[d]	4.6
	Lauryl-10	690	>0.1[d]	9.8

Table 1 : The surfactants investigated in this study.

M_n : weight, number average; n : average number of oxyethylene groups. Approximative values from ref, [62] the indicated range correspond to values obtained by different authors and/or methods. [b]CMC of Lauric acid.[63] [c]From ref[64]. [d]The CMC of the glycolic acid ethoxylate lauryl ether surfactants were not available from the literature, but are expected to be slightly larger than the one of $C_{12}E_4$.

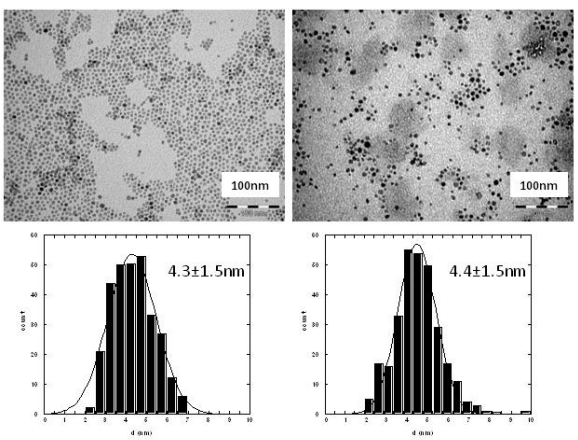

Figure 4 : TEM micrographs and size histograms of ZnO@OA Ncs (1eq) in dichloromethane (left) and after transfer to water (right) using 1mM Oleyl-10. Scale bar : 100 nm. The mean diameter is evaluated by fitting the histogram with a Gaussian curve. The first value correspond to the center of the peak whereas the second one corresponds to twice the standard deviation of the Gaussian distribution or approximately 0.849 the width of the peak at half-height.

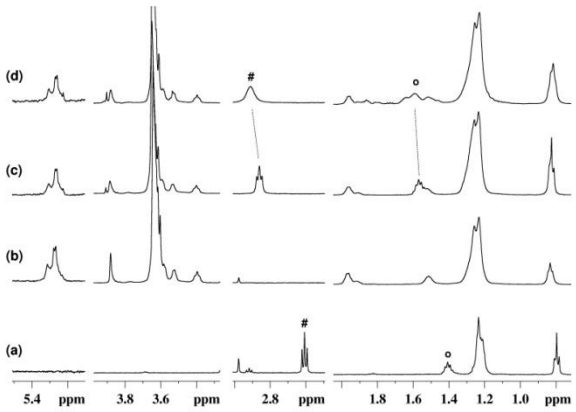

Figure 5 : ^{1}H NMR spectra in D_2O at 293K of OA at 8 mM (a); Oleyl-10 at 2 mM (b); a mixture of OA (8mM) and Oleyl-10 (2mM) (c); and ZnO/OA Nps with 2 mM of Oleyl-10 (d). Only selected areas are shown for clarity. From left to right, resonances of alkene groups of Oleyl-10, of ethylene oxide groups of Oleyl-10, of methylene in alpha position of the amine head group of OA (α-CH_2; #) and of other methylenes of OA and Oleyl-10. #: β-CH_2 of OA; Full ^{1}H spectra are shown in ESI, Figure S6.

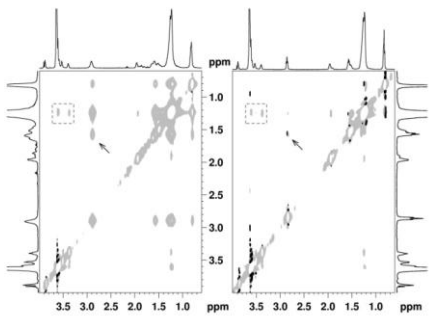

Figure 6: NOESY spectra (mixing time 100ms) in D2O at 293K of ZnO/OA Nps with 2 mM of Oleyl-10 (left) and a mixture of OA (8mM) and Oleyl-10 (2mM) (right). Arrows indicate NOE cross peaks between the α-CH2 and β-CH2 protons of OA. Boxes hightlight NOE cross peaks between protons of ethylene oxide and methylenes groups of Oleyl-10.

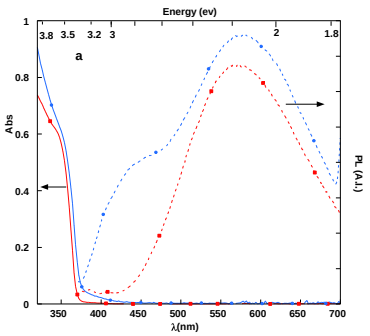

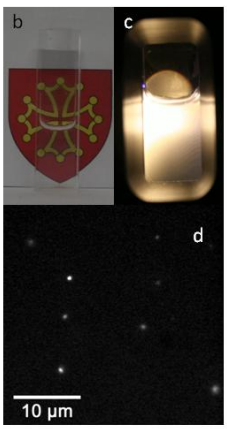

Figure 7 : (a) Absorbance and emission spectra of ZnO Ncs in dichloromethane and after transfer to water using Oleyl-10, 3 mM. Red line: Spectra in dichloromethane. Blue line: spectra in water after transfer. (b) Photograph of the transparent ZnO Ncs aqueous solution after transfer. (c) Photograph of the ZnO Ncs aqueous solution under irradiation at λ_{exc} = 360 nm. (d) Fluorescence microscopy image of ZnO Ncs in an aqueous buffer solution (Tris).

Transfer of Hydrophobic ZnO Nanocrystals to Water: an Investigation of the Transfer Mechanism and Luminescent Properties

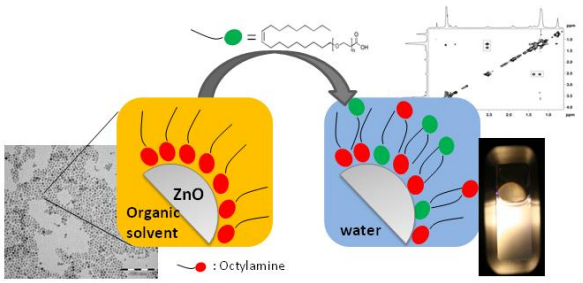

An anionic surfactant with an ethylene oxide spacer displays an unexpected ability to transfer fluorescent hydrophobic ZnO nanocrystals to water. The chemical composition of the organic interface and the optical properties of the water soluble nanocrystals were characterized.